Source of a problem with Fourier transform spectroscopy

D. B. Tanner and R. P. McCall

Thermal radiation from sample and detector can affect internally modulated Michelson interferometers (for example, rapid scanning, phase-modulated, or internally chopped) and cause serious systematic errors in the spectra measured by these instruments.

I. Introduction

In this paper we discuss an intrinsic problem with internally modulated[1] interferometers, for example, rapid-scanning Michelson interferometers,[2–9] which are commonly used in the mid-IR, and phase-modulated[1,10–16] or internally chopped[17–19] Michelson interferometers, which are frequently employed in the far IR. We show that radiation entering the interferometer from the detector port contributes to the interferogram measured by the detector and causes a systematic error in the spectrum. This error can also occur in amplitude-modulated interferometers which put the chopper in the output port.[20,21]

II. Internally Modulated Interferometers

A. Rapid-Scanning Interferometer

Rapid-scanning interferometers[2–9] that cover the mid- IR (400–4000 cm^{-1}) are produced by a number of manufacturers, for example, Analect, Bomem, Digilab, IBM, and Nicolet. These instruments are generally superior to grating or prism spectrophotometers for routine IR spectroscopy. A schematic diagram of this type of instrument is shown in Fig. 1. It consists of a lamp, a Michelson interferometer, a place to insert a sample, a detector, an audio frequency amplifier, a fast analog-to-digital converter, and a minicomputer to store the data and calculate the Fourier transform. In operation, the movable mirror is scanned at a constant velocity v making the optical path difference $x = 2vt$. The velocity is held constant by a servo loop typically involving a laser interferometer. The laser interference fringes are also used to clock the analog-to-digital converter and in some cases to maintain alignment of the interferometer.

The conventional analysis[22–24] of the electromagnetic radiation traveling through the interferometer yields for the intensity reaching the detector:

$$I(x) = \tfrac{1}{2}\int_0^\infty E_b S_L(\omega)\,d\omega + \tfrac{1}{2}\int_0^\infty E_b S_L(\omega)\cos\left(\frac{\omega x}{c}\right)d\omega, \quad (1)$$

where $S_L(\omega)$ is the intensity emitted by the lamp at angular frequency ω (as modified by transmission through or reflection by filters, windows, mirrors, samples, etc.) and E_b is the beam splitter efficiency: $E_b = 4R_b\tau_b$, with R_b the reflectance and τ_b the transmittance of the beam splitter at frequency ω. Note that in writing Eq. (1) we have neglected such complications as phase errors, finite maximum path difference, and the requirements of interferogram sampling. The first term on the right of Eq. (1) is the dc level or average value of the interferogram intensity; from now on we will denote it by I_∞. The rapid-scanning interferometer automatically suppresses this dc level because the detector is ac coupled to the amplifier.

The second term on the right of Eq. (1) is the interferogram; in the present example it is the cosine Fourier transform of the spectrum. An inverse Fourier transform of the interferogram gives the spectrum

$$E_b S_L(\omega) = \mathrm{FT}[I(x) - I_\infty] \equiv \frac{2}{\pi}\int_{-\infty}^{\infty} dx[I(x) - I_\infty]\exp(-i\omega x/c). \quad (2)$$

Here we have written the transform as a complex Fourier transform, because that is what the FFT routine usually calculates. Because the interferogram is symmetric about $x = 0$, the imaginary part is zero.

In the rapid-scanning interferometer, Fourier components of the light at angular frequency ω give a detector signal at audio frequency $f = \omega v/\pi c$. (Our Digilab spectrometer reduces 1000 cm^{-1} to ~300 Hz.) A wideband audio amplifier is used, e.g., 100–1250 Hz, to amplify the entire spectrum; sampling occurs at a 5-kHz

When this work was done both authors were with University of Florida, Physics Department, Gainesville, Florida 32611; R. P. McCall is now with University of California, Santa Barbara, Physics Department, Santa Barbara, California 93106.

Received 6 March 1984.
0003-6935/84/142363-06$02.00/0.

rate. A high SNR is achieved by repetitively scanning the interferometer mirror and coherently adding (coadding) the digitized points.[3,4,23,24] In comparison to the step-and-integrate method of Fourier spectroscopy, the rapid-scanning technique has three advantages: (1) it is less affected by lamp intensity or detector sensitivity drifts; (2) it suppresses the average value of the interferogram; and (3) it uses a simple and relatively inexpensive mirror drive mechanism.

B. Phase-Modulated Interferometer

Phase modulation[1,10–16] has been used in a number of far-IR instruments, particularly those based on the cube interferometer.[25] In these, the mirror in the fixed arm is jittered a small amount back and forth, and the detector output is phase-sensitive detected at the jitter frequency. The other mirror is slowly scanned in a stepwise fashion; at each step the detector signal is integrated to give an interferogram point.

The effect of the jitter in the fixed arm is to take the derivative with respect to the path difference of the intensity leaving the interferometer. A complete analysis[10] shows that the detector signal is the sine instead of the cosine transform of the lamp intensity:

$$I(x) = \int_0^\infty E_\phi S_L(\omega) \sin\left(\frac{\omega s}{c}\right) d\omega, \tag{3}$$

where x is the optical path difference and E_ϕ is the product of E_b and the phase-modulation efficiency factor.[10] This form of modulation automatically suppresses the average value (I_∞) term of the interferogram, giving it the advantage (compared with amplitude modulation of the source) of being less sensitive to source intensity or detector sensitivity drifts.

C. Internally Chopped Interferometer

In at least three far-IR instruments,[17–19] a chopper has been located in one of the interferometer arms. Placing the chopper in this location causes the intensity leaving the interferometer to alternate between path difference x and infinite path difference so that the average value of the interferogram is again suppressed. (We note that the interferometers of Refs. 17 and 18 have both been modified[26,27] so that the chopper is located at the source.)

D. Anti-interferogram

Each of the three cases discussed above is an internally modulated interferometer, because the modulation to which the detector amplifier responds occurs in one of the active arms of the interferometer. The main point of this paper is that this internal modulation makes the interferometer insensitive to the source of the radiation. To see this effect, first consider in Fig. 1 the intensity returned toward the lamp. This quantity is

$$I'(x) = \int_0^\infty (R_b^2 + \tau_b^2) S_L(\omega) - \tfrac{1}{2} \int_0^\infty E_b S_L(\omega) \cos\left(\frac{\omega x}{c}\right) d\omega. \tag{4}$$

The first term of Eq. (4) is an average or dc value, while the second is an inverted interferogram or anti-interferogram. Note that for a perfect beam splitter (for which $E_b = 1$ and $R_b = \tau_b = \frac{1}{2}$), $I'(0) = 0$. Clearly, from energy conservation,

$$I(x) + I'(x) = \int_0^\infty (1 - A_b)^2 S_L(\omega) d\omega, \tag{5}$$

where $A_b = 1 - R_b - \tau_b$ is the absorption by the beam splitter.

A comparison of Eqs. (1) and (4) shows that the Michelson interferometer is a device that switches energy between the detector and lamp ports; when there is a bright fringe at one port there is a dark fringe in the other and vice versa.[28–30]

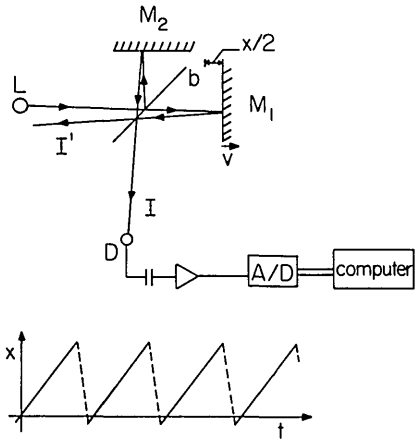

Fig. 1. Schematic diagram of a rapid-scanning Michelson interferometer. The optical components are the lamp L, beam splitter b, moving mirror M_1, fixed mirror M_2, and detector D. The detector signal is ac coupled to an audio frequency amplifier, digitized, and stored by a computer. The moving mirror moves at constant velocity v so that the optical path difference x varies linearly with time. Typically the interferometer is scanned repetitively, as indicated at the bottom of the figure, and the signals at each x value are averaged.

III. Radiation Flux in the Interferometer

If the lamp is a thermal source, its spectrum is close to that of a blackbody:

$$S(\omega) = \frac{2\hbar}{\pi c^2} \frac{\omega^3 \exp(-\hbar\omega/kT)}{1 - \exp(-\hbar\omega/kT)}, \tag{6}$$

where $T = T_L$, the temperature of the lamp. This spectrum is plotted in Fig. 2 for three values of temperature. Note that for frequency $\nu = \omega/2\pi c$ in cm^{-1} and T in kelvin, the spectra have maxima at $\nu \approx 2T$ and significant intensity (relative to the maximum) up to $\nu \approx 5T$. The limiting values for the blackbody spectrum are

$$S(\omega) = \begin{cases} \dfrac{2kT}{\pi c^2}\omega^2 & \omega \to 0, \\ \dfrac{2\hbar}{\pi c^2}\omega^3 \exp\left(-\dfrac{\hbar\omega}{kT}\right) \to 0 & \omega \to \infty. \end{cases} \tag{7}$$

Any interferometer possesses at least two sources, because the detector emits thermal radiation just as does the lamp. Consider the situation shown in Fig. 3. Light emitted by the lamp is modulated by the interferometer and reaches the detector as an interferogram,

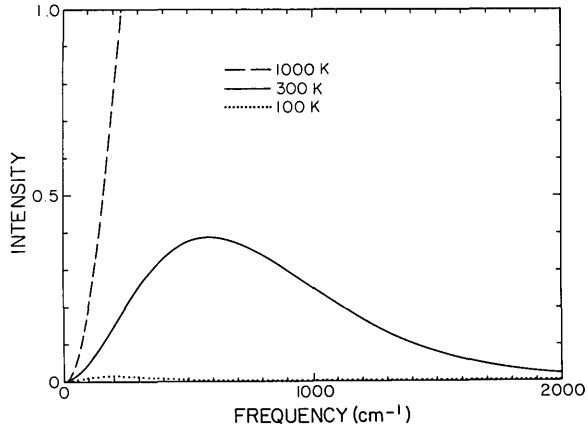

Fig. 2. Blackbody emission spectra (on an artitrary scale) vs frequency. These spectra were calculated for a constant frequency resolution of 1 cm^{-1}.

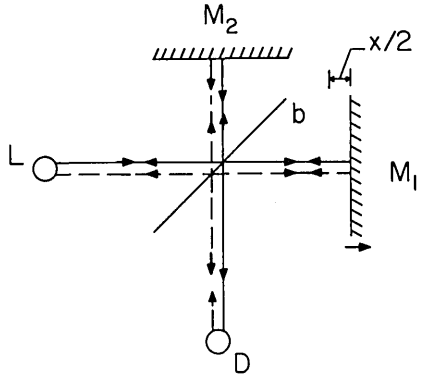

Fig. 3. Interferometer schematic showing paths taken by light from the lamp (solid line) and detector (dashed line). Both sources contribute to the detector signal in an internally modulated interferometer.

as in Eq. (1). Light emitted by the detector is modulated by the interferometer and returns to the detector as an anti-interferogram, as in Eq. (4). For simplicity we assume that $E_b = 1$ and that the lamp is a thermal source with emissivity $e_L = 1$, while the detector is a perfect receiver with absorptivity $a_D = 1$ (and hence $e_D = 1$). Thus both the lamp and detector emit blackbody spectra S_L and S_D characterized by their respective temperatures T_L and T_D. The total intensity reaching the detector is the sum of the two interferograms, or

$$I(x) = I_{L\infty} + I'_{D\infty} + \int_0^\infty [S_L(\omega) - S_D(\omega)] \cos\left(\frac{\omega x}{c}\right) d\omega, \quad (8)$$

where $I_{L\infty}$ and $I'_{D\infty}$ are dc levels.

Equation (8) is a key result of this paper. For example, intuition suggests that if an experimenter neglects to turn the source lamp, no signal will be detected. Intuition is correct, however, only so long as a room-temperature detector is used. A rapid-scanning interferometer that uses a cooled detector can give perfectly reasonable spectra when the lamp is off.

The inverse transform of the interferogram of Eq. (8).

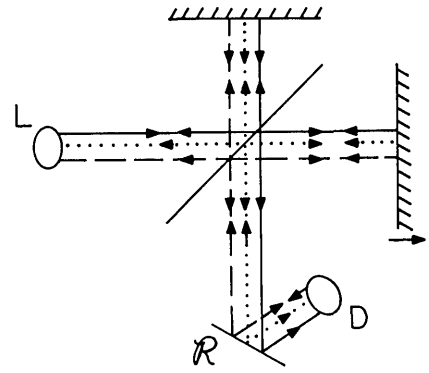

Fig. 4. Interferometer schematic showing a setup for measuring reflectance. The paths taken by light from the lamp, detector, and sample are shown, respectively, by solid, dashed, and dotted lines.

$$\mathrm{FT}[I(x) - I_\infty] = S_L - S_D \quad (9)$$

gives the difference between the two spectra.

IV. Effect of Sample

The introduction of a sample in either the source port or detector port of the interferometer affects the signal both by reducing the intensity due to the lamp and detector and by being a thermal radiation source. We consider several examples.

A. Reflection Sample

The simplest case is that of an opaque reflection sample. Figure 4 shows a schematic diagram of the typical experimental arrangement with the sample located between the interferometer and detector. The sample has reflectance $R(\omega)$ and is opaque; thus its emissivity is $e = 1 - R(\omega)$. There are three sources of radiation now: the lamp at temperature T_L and emitting a spectrum $S_L(\omega)$; the detector at temperature T_D and emitting $S_D(\omega)$; and the reflection sample at temperature T_R and emitting $eS_R(\omega)$. The light from the lamp is modulated by the interferometer, reflects off the sample, and reaches the detector. The light from the detector is reflected by the sample, is modulated by the interferometer, reflects again from the sample, and returns to the detector. The light from the sample is modulated by the interferometer, is reflected from the sample, and reaches the detector. When these three contributions are combined, the intensity reaching the detector is

$$I(x) = I_\infty + \tfrac{1}{2} \int_0^\infty [RS_L(\omega) - R^2 S_D(\omega) - eRS_R(\omega)] \cos\left(\frac{\omega x}{c}\right) d\omega, \quad (10)$$

where I_∞ is the total dc level. The inverse transform is conveniently written as

$$\mathrm{FT}[I(x) - I_\infty] = R[S_L - RS_D + (1 - R)(S_D - S_R)], \quad (11)$$

were we have used $e = 1 - R$.

A reflectance measurement is made by taking the ratio of sample spectrum, given by Eq. (11), to a background spectrum (measured by replacing the sample with a mirror having $R \approx 1$), Eq. (9). This ratio is

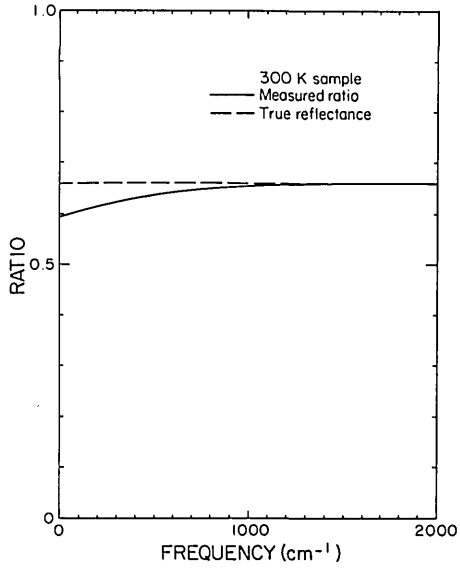

Fig. 5. Ratio of the spectrum obtained with reflectance sample to the background spectrum for the case of a cooled detector and a room temperature sample. The ratio differs from the reflectance below the 600-cm^{-1} blackbody emission peak.

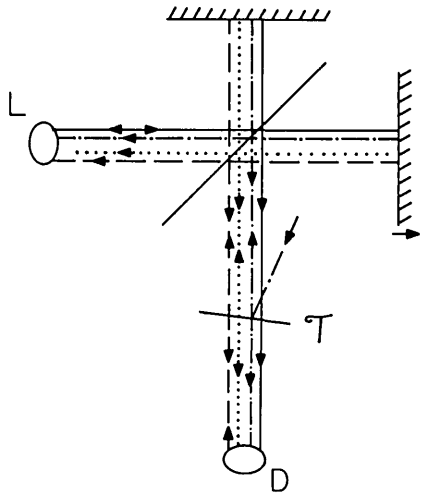

Fig. 6. Interferometer schematic showing transmission setup. Radiation from the source, detector, sample, and the ambient surroundings are shown, respectively, by solid, dashed, dotted, and dashed–dotted lines.

$$\text{ratio} = R + R(1-R)\frac{S_D - S_R}{S_L - S_D}. \tag{12}$$

If $T_D = T_R$, then ratio = R, and the measurement is accurate; otherwise it may be in error. As an example suppose $T_D \ll T_R < T_L$. Then using Eq. (7) for the limiting values of a blackbody spectrum,

$$\text{ratio} = \begin{cases} R - R(1-R)\dfrac{T_R}{T_L} & \hbar\omega \ll kT_R, \\ R & \hbar\omega \gg kT_R. \end{cases}$$

Suppose $R = 0.66$, $T_L = 1000$ K, and $T_R = 300$ K. Then at low frequencies, ratio ≈ 0.6, a 10% error! Worse, as shown in Fig. 5, which is an evaluation of Eq. (12) for the above parameters, spurious structure is introduced into the ratio at frequencies near the blackbody peak for the sample. Errors that are similar in size but with the opposite sign occur if $T_D \approx 300$ K while $T_R \ll T_D$.

B. Transmission Sample

The case of transmission sample is slightly more complicated because the sample will reflect light as well as transmit it. Its emissivity is thus $e = 1 - R - \tau$, where R is the reflectance and τ is the transmittance of the sample. If the reflected light reenters the interferometer, an error first noted by Jongbloets *et al.*[31] can occur. Briefly, light from the source which is modulated by the interferometer, reflected from the sample back into the interferometer, modulated a second time by the interferometer, and then transmitted through the sample to the detector will contribute to the interferogram as $\cos[(\omega 2x)/c]$ even though the actual phase should be $(\omega x)/c$. This light then appears to be at twice its actual frequency when the inverse transform is calculated, so that harmonics of the actual frequency are generated. Note that this error is independent of whether this modulation is internal (rapid scanning or phase modulation) or external (amplitude modulation of the source).

We will assume here that the sample reflects ambient light from the spectrometer into the interferometer, as shown in Fig. 6. There are thus four sources here: the lamp; the detector; the sample; and the ambient surroundings. By analysis similar to the previous cases,

$$\text{FT}[I(x) - I_\infty] = \tau(S_L - \tau S_D - RS_A - eS_T), \tag{13}$$

where S_T is a blackbody spectrum for the temperature of the transmission sample and S_A is a blackbody spectrum characteristic of the ambient temperature; presumably $T_A = 300$ K.

Equation (13) may be rewritten

$$\text{FT}[I(x) - I_\infty] = \tau[S_L - S_D + (1-\tau)(S_D - S_T) + R(S_T - S_A)]. \tag{14}$$

The ratio of the spectrum of the background spectrum is

$$\text{ratio} = \tau + \tau(1-\tau)\frac{S_D - S_T}{S_L - S_D} + \tau R\frac{S_T - S_A}{S_L - S_D}. \tag{15}$$

As an example, suppose $\tau = 0.4$, $R = 0.05$, $T_L = 1000$ K, $T_A = 300$ K, $T_D = 300$ K, and the sample temperature $T_\tau = 4.2$ K. With these parameters Eq. (15) is approximately

$$\text{ratio} = \begin{cases} \tau + \tau(1-R-\tau)\dfrac{T_D}{T_L - T_D} & \hbar\omega \ll kT_D, \\ \tau & \hbar\omega \gg kT_D, \end{cases}$$

or 0.48 at low frequencies, 0.4 at high frequencies. The error is ~20%, and again spurious structure is introduced into the spectrum near the room temperature blackbody peak.

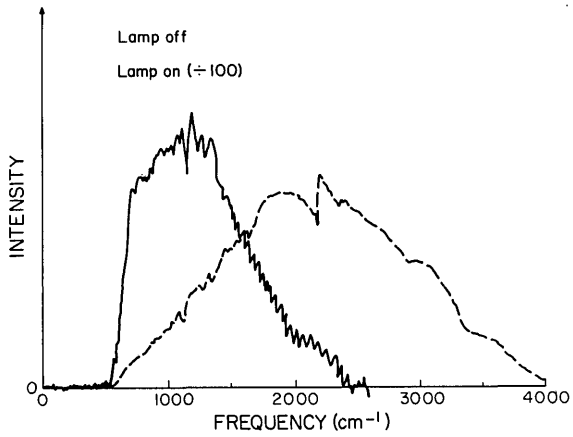

Fig. 7. Solid line gives the spectrum measured when the source lamp is turned off, and a cooled (to 6 K) transmission sample is used. Beam splitter absorption causes zero intensity below 500 cm^{-1}; otherwise the spectrum is close to that of a 300 K blackbody. The dashed line shows the spectrum when the lamp is on, divided by a factor of 100.

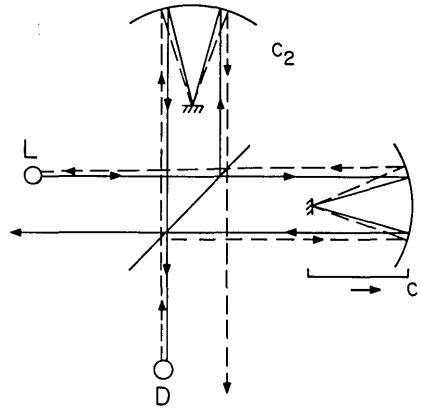

Fig. 8. Schematic diagram of an internally modulated interferometer that does not suffer from errors caused by sample or detector thermal radiation. The cat's-eye mirrors C_1 and C_2 in the active arms reflect rays across the center line of the interferometer; light emitted by the detector which returns through the detector port is not collected by the detector optics.

C. Experimental Verification

Figure 7 shows the results of our experiment to test these ideas. We used a commercial rapid-scanning interferometer[32] set up with a transmission sample as sketched in Fig. 6. The detector was operated at 300 K, while the sample was cooled to ~6 K. The solid line in Fig. 7 is the spectrum that we measured when the lamp was off. The interferometer in this case gave a signal even though both lamp and detector were at the same temperature. Following the analysis which lead to Eq. (14), this signal is

$$\begin{aligned} \mathrm{FT}[I(t) - I_\infty] &= E_B\tau(1 - R - \tau)(S_{300} - S_6) \\ &\approx E_b\tau(1 - R - \tau)S_{300}, \end{aligned} \tag{16}$$

where we have explicitly included the beam splitter efficiency E_B. The absorption by the sample has reduced the amount of 300 K radiation entering the interferometer through the detector port compared with what enters through the lamp port.

The difference between this spectrum and the 300 K blackbody spectrum is due to instrumental effects. The beam splitter, a Ge film or KBr, has zero efficiency below 500 cm^{-1} due to KBr absorption and has its maximum efficiency in the 1500–2000-cm^{-1} region.

The dashed line in Fig. 5 shows the spectrum obtained when the lamp was turned on. This spectrum has been reduced by a factor of 100; thus the ratio of signal with lamp off to signal with lamp on at 600 cm^{-1} is 0.07. According to Eq. (15) this ratio should be

$$R_{\mathrm{off/on}} = \tau(1 - R - \tau)S_{300}/S_L \approx \tau(1 - R - \tau)\frac{300}{T_L}. \tag{17}$$

The sample had $\tau = 0.4$ and $R \approx 0.05$, so that the observed ratio suggests $T_L = 950$ K, a not unreasonable value.

V. Avoiding the Problem

We can suggest two solutions to this problem. First, if the lamp is chopped (amplitude-modulated) and a lock-in amplifier is used, the signal will not be affected by emission from detector, sample, etc. since that emission is steady and thus not amplified by the lock-in. Because the bandwidth of most lock-ins is relatively limited and because chopping at very high frequencies (10–20 kHz) is difficult, this solution probably cannot be used with rapid scanning interferometers. However, phase-modulated interferometers, which operate in the step-and-integrate mode, can be corrected by changing to a chopped source. (Note that the chopper should not be located at a focal point, or it could reflect light leaving the interferometer toward the source back into the interferometer, causing errors of the kind that we have discussed here. Neither should it be located in the detector port,[20,21] where it would modulate radiation entering the interferometer from the detector.)

Figure 8 suggests a solution suitable for rapid-scanning instruments. The mirrors at the end of the active arms are cat's-eyes or rooftop mirrors,[28] either of which return rays on the opposite side of the system axis from the one the rays entered. The detector optics are arranged so that light emitted from the detector or sample into the interferometer is not returned to the detector. Although this design eliminates the problem, it clearly adds to the cost and complexity of the interferometer. The beam splitter must be twice as large as before because different halves of it are used as input and output beam splitters. The added weight of the moving cat's-eye or rooftop mirror may increase the cost of the drive mechanism. Finally, on account of the added complexity of the interferometer, alignment will be substantially more difficult.

VI. Conclusion

Not knowing the source of the radiation being detected causes problems for three kinds of Fourier transform spectrometers. All three are characterized by internal modulation of the interferogram: rapid-scanning interferometers, phase-modulated instruments and amplitude modulation in one of the active arms. The lack of discrimination introduces significant errors into measurements of transmission and reflection; errors occur both in the magnitude and shape of the curves. Errors are seen at all frequencies where there is thermal radiation from samples or optical components (other than the lamp which is intended to be the source), i.e., for $\nu < 5T_{\max}$, where ν is in cm^{-1} and

T_{max} is the highest temperature (in kelvins) of these other sources.

We have three final comments. First, lamelar grating interferometers[33] do not suffer from this effect, because they operate by switching energy between the zero order and higher orders of diffraction instead of between detector and source ports. Second, dual-beam spectrophotometers which use optical nulling are also affected by thermal emission from the sample, because the chopper is usually also the beam combiner and thus chops thermal radiation from the sample and the reference beam attenuator as well as from the lamp. When sample and reference beam attenuator are at different temperatures, the null will occur at an incorrect value of transmittance; this error actually can lead to negative measured transmittance. It can be compensated for only by readjusting the balance point of the spectrophotometer at each frequency. Third, the cure suggested by Fig. 8 also will correct the error described by Jongbloets *et al.*,[31] because light reflected from the sample is not allowed to return to the detector.

This research was supported by the National Science Foundation, Solid State Chemistry, through grant DMR-8218021.

References

1. J. Connes and P. Connes, "Near-IR Planetary Spectra by Fourier Spectroscopy," J. Opt. Soc. Am. **56,** 896 (1966).
2. L. Genzel and R. Weber, "Zur Theorie der Interferenz-Modulation für Zweistral-Interferenzen," Z. Angew. Phys. **10,** 127 (1958); "Spectroskopie im Fernen Ultrarot durch Interferenz-Modulation," Z. Angew. Phys. **10,** 195 (1958).
3. L. Mertz, *Transformations in Optics* (Wiley, New York, 1965); L. Mertz, J. Phys. Colloid Chem. C2, Suppl. 3–4 **28,** 88 (1967).
4. D. M. Hunten, "Fourier Spectroscopy of Planets," Science **162,** 313 (1968).
5. J. Cuthbert, "Fourier Transform Spectroscopy," J. Phys. E **7,** 328 (1974).
6. G. Horlick and W. K. Yuen, "A Modular Michelson Interferometer for Fourier Transform Spectrochemical Measurements from the Mid-infrared to the Ultraviolet," Appl. Spectrosc. **32,** 38 (1978).
7. A. A. Balashov, V. S. Bukreev, N. G. Kultepin, I. N. Nesteruk, E. B. Perminov, V. A. Vagin, and G. N. Zhizhin, "High-Resolution Fourier Transform Spectrometer (0.005-cm^{-1}) for the 0.6–100-μm Spectral Range," Appl. Opt. **17,** 1716 (1978).
8. R. P. Walker and J. D. Rex, "Interferometer Design and Data Handling in a High-Vibration Environment. Part I: Interferometer Design," Proc. Soc. Photo-Opt. Instrum. Eng. **191,** 88 (1979).
9. W. M. Doyle, B. C. McIntosh, and W. L. Clark, "Refractively Scanned Interferometers for Fourier Transform Infrared Spectrophotometry," Appl. Spectrosc. **34,** 599 (1980).
10. J. E. Chamberlain, "Phase Modulation in Far Infrared (Submillimetre Wave) Interferometers. I Mathematical Formulation," Infrared Phys. **11,** 25 (1971).
11. J. E. Chamberlain and H. A. Gebbie, "Phase Modulation in Far Infrared (Submillimetre Wave) Interferometers. II Fourier Spectroscopy and Terametrology," Infrared Phys. **11,** 57 (1971); "Use of Phase Modulation in Submillimeter-Wave Interferometers," Appl. Opt. **10,** 1184 (1971).
12. T. J. Parker and W. G. Chambers, "Measurements of the Complex Far Infrared Reflectivity of KBr at 100 and 300 K," Infrared Phys. **16,** 349 (1976).
13. J. R. Birch, G. D. Price, and J. E. Chamberlain, "Dispersive Fourier Transform Measurements on Opaque Solids from 5 to 350 cm^{-1}," Infrared Phys. **16,** 311 (1976).
14. M. N. Afsar, J. B. Hasted, and J. Chamberlain, "New Techniques for Dispersive Fourier Transform Spectroscopy of Liquids," Infrared Phys. **16,** 301 (1976).
15. J. R. Birch and D. K. Murray, "A Modular Interferometer for Dispersive Reflectivity Measurements on Highly Absorbing Solids," Infrared Phys. **18,** 283 (1978).
16. M. N. Asfar and K. J. Button, "Millimeter and Submillimeter Wave Measurements of Complex Optical and Dielectric Parameters of Materials: I. 2.5 mm to 0.66 mm for Alumina 995, Beryllia, Fused Silica, Borosilicate and Glass Ceramic," Int. J. Infrared Millimeter Waves **2,** 1029 (1981); "II. 5 mm to 0.66 mm for Corning Macor Machinable Glass Ceramic and Corning 9616 Green Glass," Int. J. Infrared Millimeter Waves, **3,** 929 (1982).
17. E. E. Russell and E. E. Bell, "Measurements of the Far Infrared Optical Properties of Solids with a Michelson Interferometer Used in the Asymmetric Mode: Part II, the Vacuum Interferometer," Infrared Phys. **6,** 75 (1966).
18. R. B. Sanderson and H. E. Scott, "High Resolution Far IR Interferometer," Appl. Opt. **3,** 1097 (1971).
19. G. Bachet and R. Coulon, "New Modular Interferometer for Fourier Transform Spectroscopy at High Resolution in Far Infrared," Infrared Phys. **17,** 359 (1977).
20. P. L. Richards, "High-Resolution Fourier-Transform Spectroscopy," J. Opt. Soc. Am. **54,** 1474 (1964).
21. J. Kauppinen, "Double-Beam High Resolution Fourier Spectrometer for the Far Infrared," Appl. Opt. **14,** 1987 (1975); "Working Resolution of 0.0100 cm^{-1} Between 20 cm^{-1} and 1200 cm^{-1} by a Fourier Spectrometer," **18,** 1788 (1979).
22. A. E. Martin, *Infrared Interferometric Spectrometers* (Elsevier, Amsterdam, 1980).
23. R. J. Bell, *Introductory Fourier Transform Spectroscopy* (Academic, New York, 1972).
24. P. R. Griffiths, *Chemical Infrared Fourier Transform Spectroscopy* (Wiley, New York, 1975).
25. G. W. Chantry, H. M. Evans, J. Chamberlain, and H. A. Gebbie, "Absorption and Dispersion Studies in the Range 10–1000 cm^{-1} Using a Modular Michelson Interferometer," Infrared Phys. **9,** 85 (1969).
26. K. D. Cummings and D. B. Tanner, "Far-Infrared Ordinary-Ray Optical Constants of Quartz," J. Opt. Soc. Am. **70,** 123 (1980).
27. K. D. Cummings, D. B. Tanner, and Joel S. Miller, "Optical Properties of Cesium Tetracyanoquinodimethanide, $Cs_2(TCNO)_3$," Phys. Rev. B **24,** 4142 (1981).
28. W. J. Burroughs and J. Chamberlain, "Submillimeter-Wave Solar Observation Using a Double-Output Michelson Interferometer," Infrared Phys. **11,** 1 (1971).
29. H. R. Chandresekhar, L. Genzel, and J. Kuhl, "Double-Beam Fourier Spectrometer with Inteferometric Background Compensation," Opt. Commun. **17,** 106 (1976); L. Genzel, H. R. Chandresekhar, and J. Kuhl, "Double-Beam Fourier Spectroscopy with Two Inputs and Two Outputs," Opt. Commun. **18,** 381 (1976).
30. The two input and two output ports of the Michelson interferometer are discussed in detail by D. H. Martin, in *Infrared and Millimeter Waves, Vol. 6,* K. H. Button, Ed. (Academic, New York, 1982), p. 65.
31. H. W. H. M. Jongbloets, M. J. H. vande Steeg, E. J. C. M. van der Werf, J. H. M. Stoelinga, and P. Wyder, "Spectrum Distortion in Far-Infrared Fourier Spectroscopy by Multiple Reflections Between Sample and Michelson Interferometer," Infrared Phys. **20,** 185 (1980).
32. Digilab FTS-14
33. J. Strong and G. Vanasse, "Lamellar Grating Far-Infrared Interferometers," J. Opt. Soc. Am. **50,** 113 (1960).